Grain Refinement and Improvement of Solidification Defects in Direct-Chill Cast Billets of A4032 Alloy by Melt Conditioning

HU-TIAN LI, PIZHI ZHAO, RONGDONG YANG, JAYESH B. PATEL, XIANGFU CHEN, and ZHONGYUN FAN

Melt-conditioned, direct-chill (MC-DC) casting is an emerging technology to manipulate the solidification process by melt conditioning *via* intensive shearing in the sump during DC casting to tailor the solidification microstructure and defect formation. When using MC-DC casting technology in an industrial scale DC cast billet of an A4032 aluminum alloy, significant grain refinement and uniform microstructure can be achieved in the primary α-Al phase with fine secondary dendritic arm spacing (SDAS). Improved macrosegregation is quantitatively characterized and correlated with the suppression of channel segregation. The mechanisms for the prevention of channel segregation are attributed to the increased local cooling rate in the liquid–solid phase region in the sump and the formation of fine equiaxed dendritic grains under intensive melt shearing during MC-DC casting. A critical cooling rate has been identified to be around 0.5 to 1 K/s (°C/s) for the channel segregation to happen in the investigated alloy based on quantitative metallographic results of SDAS. Reduction and refinement of microporosity is attributed to the improved permeability in the liquid–solid phase region estimated by the Kozeny–Carman relationship. The potential improvement in the mechanical properties achievable in MC-DC cast billets is indicated by the finer and more uniform forging streamline in the forgings of MC-DC cast billet.

DOI: 10.1007/s11663-017-1016-7

I. INTRODUCTION

IN direct chill (DC) casting of Al alloys, a grain-refined as-cast microstructure is generally desirable. McCartney has defined grain refinement as deliberate suppression of columnar grain growth in castings and formation of a fine equiaxed solidification structure throughout the material.[1] Effective grain refinement brings many direct and indirect benefits, including the possibility of faster production of DC castings. During DC casting, grain refinement directly affects the formation of porosity, the tendency of hot tearing, the pattern of macro-segregation, and the scale of micro-segregation. Grain refinement also influences the mechanical properties of solidified material, the kinetics of homogenization treatment, the formability and defect formation during downstream thermomechanical processing, and anodizing quality.[1–3] Al-Ti-B master alloys are commonly used as grain refiners during DC casting of wrought Al alloys in the industry. Nevertheless, less than 1 pct of the added TiB_2 particles (nuclei particles in Al-Ti-B master alloys) are active for nucleation of the α-Al phase.[2] On the other hand, the presence of solute is not always beneficial to grain refinement; the solute can interact with TiB_2 particles rendering them ineffective during the nucleation process. This is the so-called poisoning effect on grain refinement.[4–9] In Al-Si cast alloys, when the Si content exceeds ~2 wt pct, a poisoning effect is observed and it becomes worse with increased Si content. When Si content is greater than 3 wt pct, the grain refining efficiency of commercial Al-Ti-B master alloys is poor.[4–9] With the increase in billet size and resulting increase in solidification time, equiaxed grain settling becomes more important in determining the columnar to equiaxed transition (CET) and, therefore, grain refinement. This makes the achieving grain refinement even more challenging. The other issue is the nonuniform microstructure that forms across the cross section of the billet. The structure that forms in

HU-TIAN LI, JAYESH B. PATEL, and ZHONGYUN FAN are with BCAST, Brunel University London, Uxbridge, Middlesex UB8 3PH, U.K. Contact e-mails: hu-tian.li@brunel.ac.uk, john.li2009@gmail.com PIZHI ZHAO is with Chinalco Materials Application Research Institute Co., Ltd., Beijing 100082, P.R. China. RONGDONG YANG and XIANGFU CHEN are with the Southwest Aluminum (Group) Co., CHINALCO, Chongqing 401326, P.R. China.

Manuscript submitted December 12, 2016.
Article published online June 26, 2017.

different zones of the billet depends on their chemical composition and local cooling rate. The local cooling rate (dT/dt) varies from 0.4 to 1 K/s (°C/s) in the center of the billet to around 10 to 20 K/s (°C/s) in the surface zone.[10] In industrial practice, even with the grain refiner (Al-Ti-B master alloy) or modifier (Al-Sr master alloy) additions, direct-chill cast billets of near eutectic Al-Si alloys, such as A4032 alloy, display severe nonuniform microstructures consisting of a coarse dendritic primary α-Al phase and coarse blocks and acicular/flake-like particles of primary and eutectic Si phases, as well as of coarse intermetallic particles. These coarse Si/intermetallic phases can easily give rise to stress concentrations and cause micro-cracks during the thermal mechanical deformation process, which will seriously deteriorate the mechanical properties and processability of these alloys. The other issue is the severe macrosegregation, which refers to the variation of composition on a large scale across the whole cross section of the casting and cannot be eliminated only by a simple modification of DC casting process parameters, but also it cannot be removed even with a long homogenization process, and have to be controlled and minimized during the solidification process.[10–16] Although extensive effort has been devoted to understanding the underlying mechanisms of macrosegregation, limited successes have been reported to alleviate the macrosegregation in large-sized DC cast billets/ingots.[17–20] For Al-Si near eutectic alloy, as a result of the high Si content and thus difficulties in grain refinement of the α-Al phase, controlling of macrosegregation is more challenging. Microporosity is another concern for large-sized DC cast billets that can give rise to stress concentrations and early failure during thermomechanical deformation. The microporosity present in the DC cast ingot is usually removed during the thermomechanical deformation, as a result of the very high compressive strains involved. Nevertheless, this may not be complete. For high-strength Al alloys used for applications requiring exact tolerances, porosity in the final product may still reduce the final mechanical properties.

Melt-conditioned direct chill (MC-DC) casting is an emerging technology that optimizes the solidification process during DC casting for *in situ* microstructural control.[21–28] The MC-DC casting process combines conventional vertical DC casting with high shear melt conditioning directly in the sump of DC casting to manipulate the solidification microstructure and defect formation of the resultant cast billets/ingots (Figure 1). Intensive melt shearing in the sump has the following effects: (1) effective breakup, dispersion, and uniform distribution of solid particles in the alloy melt (such as oxide films and other inclusions), which can act as nucleation sites and enhance heterogeneous nucleation during the solidification process[23–26]; and (2) intensive melt convection enhances mass transport and thermal exchange in such a way to shape the sump profile with shallow sump depth.[22,27] In this article, the effect of intensive melt shearing in the sump during MC-DC casting process on the evolution of grain structure and solidification defects, such as macrosegregation and porosity, have been investigated. The mechanisms underlying the grain structure evolution and formation of solidification defects are discussed based on a semiquantitative analysis of the thermal conditions and permeability in the liquid–solid phase region in the sump.

II. EXPERIMENTAL

The alloy investigated was A4032 (compositions all in wt pct): Si: 11.6, Mg: 1.07, Ni: 0.92, Cu: 0.87, Fe: ≤0.21, Zn: ≤0.1, Al: remaining, calculated liquidus temperature ~850 K (577 °C). A vertical DC caster with open hot top was used. The dimensions of DC cast billets were 650 mm diameter and 4,610 mm in length. In the case of grain refiner (GR) added, 1.4 kg/ton Al-5Ti-1B master alloy was added to the alloy melt in the launder prior to being poured into the DC caster system. The melt temperature in the launder was 973 K (700 °C). For MC-DC casting, an 80-mm-diameter high shear device was positioned in the middle of the hot-top DC caster system at a predetermined height, running at a rotation speed of 1500 rpm. DC casting speed was set at 60 mm/min. The samples for macro- and micro-structural observation and compositional analysis were cut from the edge to the center of the 650-mm-diameter billet after a stress relief heat treatment. The positions where samples were cut are shown in Figure 2. The samples for macrostructural comparison were etched by 10 wt pct NaOH water solution. The samples for microstructural examination were cut from five locations, 10, 80, 160, 240, and 320 mm, from the edge of billets.

The grain structures of the α-Al phase in all samples were examined with a Zeiss optical microscope after preparation using the standard metallographic techniques, ground, polished, and then anodized at 20 V using direct current electrical supply in a 3 to 4 pct HBF_4 water solution. The statistical analysis of the grain size and secondary dendrite arm spacing (SDAS) was carried out on the optical micrographs taken under polarized light. For columnar dendrites, grain size refers to the length of dendritic trunks. For equiaxed dendrites, grain size was measured using the linear intercept technique (ASTM 112-96). In each case, at least 200 grains or dendrite trunks on randomly taken fields of view were examined. The SDAS was measured by finding several adjacent dendrite arms from one primary dendrite arm and measuring the distance between the dendrite arm centers. At least five fields of view were analyzed for each measurement, with approximately 50 secondary dendrite arms from multiple primary dendrite arms being counted in each field of view. Average size and area fraction of microporosity were measured, on micrographs magnified at 100 times taken from the samples from central portion of DC and MC-DC cast billets, using a Zeiss optical microscope equipped with an AxioVision 4.3 quantimet digital image analysis software. The compositional analysis from the edge to the center was carried out with optical emission spectroscopy (OES) on a Foundry Master Pro analyzer. Chemical composition was measured on samples 15 mm

wide and high that were cut from the vertical section of the billet. Measurement was done at an interval of 10 mm, starting from the point 5 mm from the surface of a billet toward the center. With use of a CALPHAD software package based on the Scheil-Gulliver model, solute concentration of the interdendritic liquid against solid fraction of A4032 alloy was estimated during solidification.

III. RESULTS

A. *Grain Refinement and Uniformity of Grain Structure*

In conventional direct chill cast billets of A4032 alloy, even with grain refiner additions (Al-Ti-B-Sr), the as-cast structure displays coarse and nonuniform structures consisting of coarse dendritic primary α-Al phase and blocks/flakes of eutectics. Figure 3 shows the macrostructure of DC cast billets made under different conditions. In general, from edge to center, the structure becomes coarser for each billet. It is most significant in the case of conventional DC casting of A4032 alloy (Figures 3(a) and (b)), and it is far less significant in the case of MC-DC cast billets (Figures 3(c) and (d)). In the following section, it will be seen that the black regions on these images correspond to eutectic rich zone, which will be correlated with the nonuniform distribution of cooling rate and the formation of channel segregation.

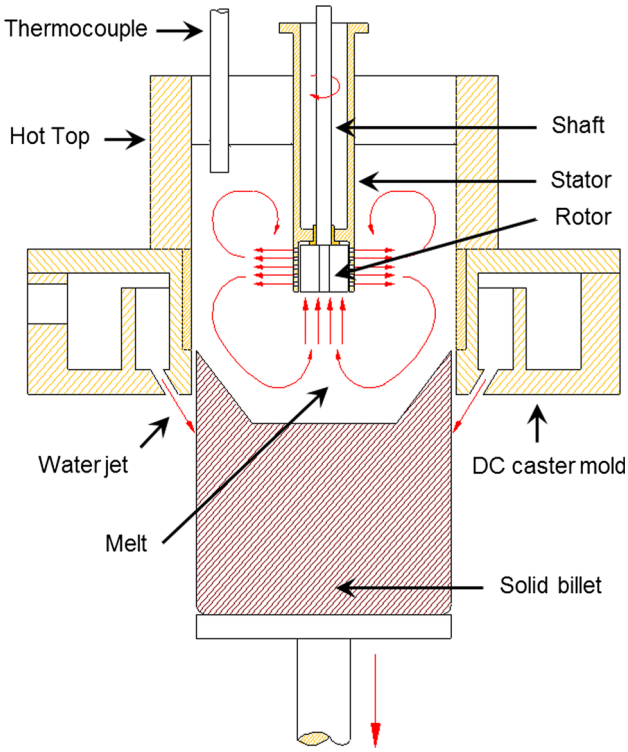

Fig. 1—Schematic representation of the arrangement of MC-DC casting. In a vertical hot-top direct chill (DC) caster, a rotor–stator high shear device located at a predetermined height in the center along the vertical axis of the mould and hot-top assembly of a vertical DC caster.

Figure 4 compares the grain structure of the α-Al phase in all samples of A4032 alloy in the central portion, where the cooling rate was low. In Figure 4(c), grain 1 and grain 2 are distinguished based on the difference in color (contrast). Caution should be taken when counting the number of grains as a result of the anodized shading that occur on the eutectics. A transition from coarse columnar dendrites in conventional DC cast billets (Figures 4(a) and (b)) to fine equiaxed dendrites in MC-DC cast billets was observed (Figures 4(c) and (d)), and significant grain refinement of the α-Al phase was achieved in MC-DC cast billets.

In conventional DC casting, in general, from edge to the center, the cooling rate decreases. So the grain size becomes coarser close to the center (Figure 5). In MC-DC cast billet, however, uniform grain size across the cross section is revealed in Figure 5.

The refining of secondary dendritic arm spacing (SDAS) in DC castings is more important for the distribution of microporosity and for intermetallic particles that form at the late stages of solidification. The refinement of SDAS of the α-Al phase in MC-DC cast billet is demonstrated by the quantification results shown in Figure 6. The values of SDAS in conventional DC and MC-DC cast billets at five locations from edge to center, 10, 80, 160, 240, and 320 mm, from the billet surface to the center are shown in Figure 6(a). The values of SDAS increase with the increased distance from the billet edge for both billets. Nevertheless, at each location in the MC-DC cast billet, it has a finer structure compared with the conventional DC cast billet. Figure 6(b) compares the values of SDAS of the samples 320 mm from the billet surface (central portion) of all billets investigated. Again, SDAS values of MC-DC cast billets are much finer than those of conventional DC cast billets.

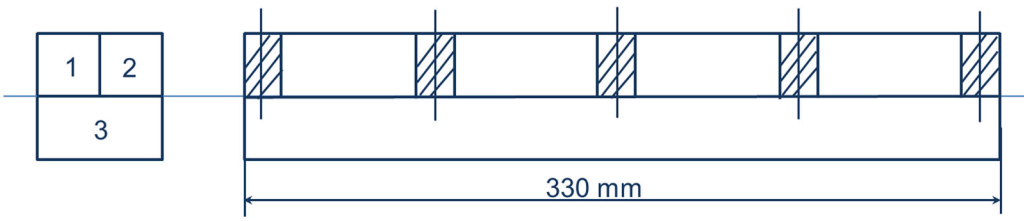

Fig. 2—Schematic of the samples cut from DC and MC-DC cast billets from edge to center: 1—samples for compositional analysis (across the cross section); 2—samples for microstructural examination (five samples examined for each condition, 10, 80, 160, 240, and 320 mm from the edge, respectively.); and 3—samples for macrostructural comparisons: from edge to center.

B. *Reduced Content and Refinement of Microporosity*

Although the microporosity found in the DC cast billets might be eliminated during the thermomechanical deformation as a result of the very high compressive strains involved, for high-strength Al alloys used for applications requiring exact tolerances, the porosity in the final product may still reduce the mechanical properties. Figure 7 compares the features of microporosity in DC and MC-DC cast billets. Both types of samples were sectioned in the central portion of the billet, where a lower cooling rate is normally experienced. Clusters of porosity can be observed on 2-D micrographs (Figure 7(a)). In 3-D, they are more likely to be tortuous channels of pores associated with eutectic networks. It can be seen that the size of shrinkage porosity was significantly refined in the MC-DC cast billet (Figure 7(b)) compared with those in a conventional DC cast billet (Figure 7(a)). In Figure 7(c), an almost round pore is observed in the MC-DC cast billet, which is more likely to be gas porosity. In Figure 8, one can see the refinement in the size of microporosity in the MC-DC cast billet, and the reduction in the content (area fraction) of microporosity, from 0.4 pct in the conventional DC cast billet down to 0.15 pct in the MC-DC cast billet. The large gas porosities (as shown in Figure 7(c)) contributed significantly to the average size of microporosity as a whole (Figure 8).

C. *Channel Segregation and Alleviated Macrosegregation by MC-DC Casting*

In the DC cast billet of eutectic Al-Si alloys (*e.g.*, A4032 alloy in the present study), achieving uniform distribution of the constituent phases has been a challenge. During the DC casting process, more than 80 pct of the total heat from the alloy melt is extracted through secondary cooling.[29] The local cooling rate depends on both the heat transfer through water spray directly impinging onto the billet surface that mainly influence the surface temperature of the billet and the heat exchange mechanism inside the sump. The local cooling rate experienced in a commercial-sized DC cast billets/ingot varies from 0.4-1 to 10-20 K/s (°C/s).[10] The large differences in cooling rates across the section of billets result in the nonuniform distribution of grain size. In particular, channel segregation occurs when a coarse columnar dendritic structure forms.

Figure 9 illustrates an example of the formation of channel segregation, showing nonuniform distribution of primary α-Al phase and eutectic structures in conventional DC cast billets of an A4032 alloy. It features mainly a eutectic structure with a few dendritic fragments marked with white loops in Figure 9(b). The dendritic fragments in Figure 9(b) are the residual from remelting caused by the interdendritic fluid flow during the development of the channel. These eutectic-rich zones can be large, up to centimeters in length, and correspond to the black regions observed on the macrographs (Figures 3(a) and (b)). This phenomenon results in severe macrosegregation, as shown in Figures 10 and 11.

Figures 10 and 11 reveal the alleviation of macrosegregation in MC-DC cast billets of an A4032 alloy. To clarify the macrosegregation, relative concentration (*e.g.*, for Si, ([Si] – [Si]nominal)/[Si]nominal) was plotted against the locations along the radial direction from the edge of the billet toward center to reveal the variation of concentration across the section. The MC-DC castings show improvement in macrosegregation regardless of whether a grain refiner was added. More interestingly, the MC-DC cast billet without grain refiner shows the best improvement in macrosegregation (Figure 10). This is consistent with the observation that the MC-DC cast billet without grain refiner shows the most uniform macrostructure and is nearly free of channel segregation (Figure 3(d)).

To investigate the technical advantages achieved with MC-DC casting technology, the cast billets were homogenized and forged. Figure 12 compares the evolution of forging streamline in forgings of DC and MC-DC cast billets. The forging streamline in forgings of the MC-DC cast billet is finer and more uniform (Figure 12(a)), in contrast to the coarse and nonuniform streamline observed in conventional DC casting (Figure 12(b)). This difference indicates the potential improvement in mechanical properties achieved in MC-DC cast billets and will be presented in a future contribution.

IV. DISCUSSION

A. *Significant Refinement and Improved Uniformity of Grain Structure*

The grain size is determined by the combined effect of nucleation (normally combined with dendrite fragmentation) and growth determined by local cooling rate and flow convection. For the investigated alloy, the dominant naturally occurring oxide in the melt should be $MgAl_2O_4$, which has been identified to be very potent nucleating particles for the α-Al phase.[25,26] In consideration of the significantly increased number density of oxide particles, ascribing to the dispersion effect by high shear mechanism,[23–26] the melt conditioning in the sump during DC casting enhances heterogeneous nucleation on dispersed oxide particles for grain refinement even without deliberate addition of grain refiner. In addition, as a result of intensive shearing, fragmentation of dendritic grains from the lower portion of the sump could also contribute to enhanced nucleation and thus grain refinement achieved in MC-DC cast billets. In contrast, in conventional DC casting with Al-Ti-B-Sr addition, the grain refining effect is not ideally achieved as a result of the poisoning caused by the high Si content in the investigated alloy (Figures 4 and 5).

In conventional DC casting, in general, the cooling rate decreases from the edge to the center of the billet. The cooling rate experienced in a commercial-sized DC cast ingot varies from 0.4-1 to 10-20 K/s (°C/s).[10] The distributions of cooling rates across the section of billets result in the nonuniform distribution of grain size.[10] In

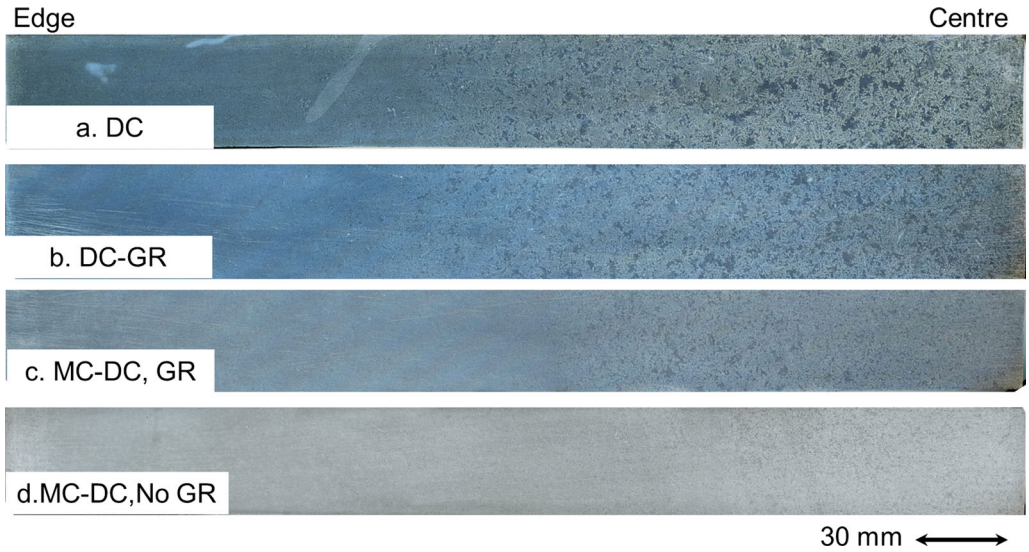

Fig. 3—Macrographs of DC and MC-DC castings, from edge to center, showing the nonuniform structures with a coarser structure being mainly observed in the areas close to the center in conventional DC cast billets (*a*) and (*b*); In MC-DC cast billets (*c*) and (*d*), an almost uniform structure can be observed, in particular, in the MC-DC cast billet without grain refiner addition (*d*).

the MC-DC cast billet, however, a uniform grain size across the cross section is revealed in Figure 5.

Based on the measured SDAS values shown in Figure 6(a), the average local cooling rate in the sump can be estimated using the following empirical equation[30]:

$$\log\frac{\mathrm{d}T}{\mathrm{d}t} = -\left(\frac{\log(DAS) - 1.66}{0.40}\right) \qquad [1]$$

where the secondary DAS is in μm and dT/dt is the local cooling rate (K/s, °C/s). The calculated local cooling rate in the sump of the conventional DC and MC-DC cast billets with grain refiner addition is given in Figure 13. This indicates that the cooling rate during MC-DC casting nearly doubles that of conventional DC casting.

The cooling rate during DC casting represents the heat extraction rate when passing the solidification range defined by liquidus and solidus. The local cooling rate at different locations in the sump depends on the heat transfer mechanism both on the surface by secondary cooling and mass transfer, thus, the heat exchange mode locally inside the liquid–solid zone in the sump. The heat transfer mechanism achieved through secondary water cooling can be distinguished by four categories, which depends on the surface temperature of the billet when the secondary cooling water impinges the billet surface.[29] In order of increasing surface temperature, they are convective cooling, nuclei boiling, transition boiling, and film boiling. From practical casting experience, the heat transfer on the billet surface by a nuclei boiling mechanism is dominant during the steady-state casting phase.[31] Under a given DC casting condition, the local cooling rate in the sump depends on the mass transfer and, thus, the heat exchange mode locally in the sump. The forced convection present during MC-DC casting enhances the mass transfer/heat extraction rate; therefore, increasing the cooling rate in the sump is expected compared with that of the conventional DC casting. In a previous study, A1-Si alloy ingots were directionally solidified vertically in a rectangular cavity with bulk liquid flow stirred with a controllable electromagnetic stirrer.[32] Temperature measurements during solidification showed that the electromagnetic stirring resulted in rapid removal of bulk liquid superheat. This is similar to the case in the present study, where forced convection results in a higher cooling rate in the liquid–solid phase region of the sump.

In summary, enhanced nucleation by dispersed oxide particles and dendrite fragmentation in combination with an increased cooling rate in the sump resulted in the refinement and uniform grain structure across the cross section of the MC-DC cast billets.

B. *Reduction and Refinement of Microporosity*

As reported by Campbell, porosity is associated with a hydrostatic depression in the mushy zone combined with segregation of gaseous solute elements (hydrogen, nitrogen, and carbon monoxide).[33] So porosity formation during solidification of aluminum alloys has two primary causes: (1) inefficient interdendritic liquid metal feeding of the alloy's volumetric shrinkage resulting in the shrinkage porosity; and (2) reduced solubility of dissolved hydrogen in the alloy upon solidification resulting in the so-called gas porosity.[34] The rate at which a viscous fluid flow through a porous medium is proportional to the pressure gradient, and the constant of proportionality, is the permeability K, also called Darcy's constant. In columnar dendrites, the permeability is affected by the direction of flow; the value of permeability for a flow parallel to the primary dendrite arms is different from that for the flow normal to the primary dendrite arms. So the permeability of the flow

through a columnar dendritic structure is anisotropic. It should be noted that the Kozeny–Carman relationship could be expressed in different ways depending on which grain structure parameter is most important for the estimation of permeability.[10] For simplicity, as far as the permeability of the interdendritic flow parallel to the primary dendrite arms is concerned, the permeability can be estimated using the modified Kozeny–Carman relationship as follows[35]:

$$K_1 = \frac{\lambda_2^2}{180}\frac{(1-f_s)^3}{f_s^2} \quad [2]$$

where λ_2 is the secondary dendrite arm spacing and f_s is the solid fraction. In the case of fine equiaxed grains, adopting the model of an isotropic porous media for equiaxed grains or spherical grains, the permeability of the flow in the mushy zone can be estimated using the modified Kozeny–Carman relationship as follows[36]:

$$K_2 = \frac{d^2}{180}\frac{(1-f_s)^3}{f_s^2} \quad [3]$$

where d is the grain size of the equiaxed grains and f_s is the solid fraction. When the secondary dendrite arm spacing of 95 μm for columnar dendrites in conventional DC cast billets (Figure 6), and the average grain size of 650 μm in MC-DC cast billets (Figure 5), both with and without grain refiner additions, is taken into account, the permeability of the flow in the mushy zone, K, with different grain morphologies is as estimated and compared in Figure 14.

As shown in Figure 14, the permeability of the mushy zone flow in MC-DC casting is much higher than that in conventional DC casting. This is the reason for the improved interdendritic feeding. The reduced porosity content and refinement of size of microporosity can be attributed to the improved permeability. The resulting improvement in feeding capability in the mushy zone is a result of a transition from coarse columnar dendrites in conventional DC cast billets to fine equiaxed dendritic grains in MC-DC cast billets.

Nevertheless, it is important to mention that it is often the larger pore size that is the limiting factor for the mechanical properties rather than the percentage and average size of microporosity.[34] Therefore, although the size and content of microporosity can be reduced through MC-DC casting technology, the degassing process prior to DC casting should be improved to reduce the population of microporosity further, in particular, the large gas porosity (Figure 7(c)).

C. *Alleviated Macrosegregation by MC-DC Casting*

Macrosegregation originates from microsegregation-partitioning behavior of solute elements between

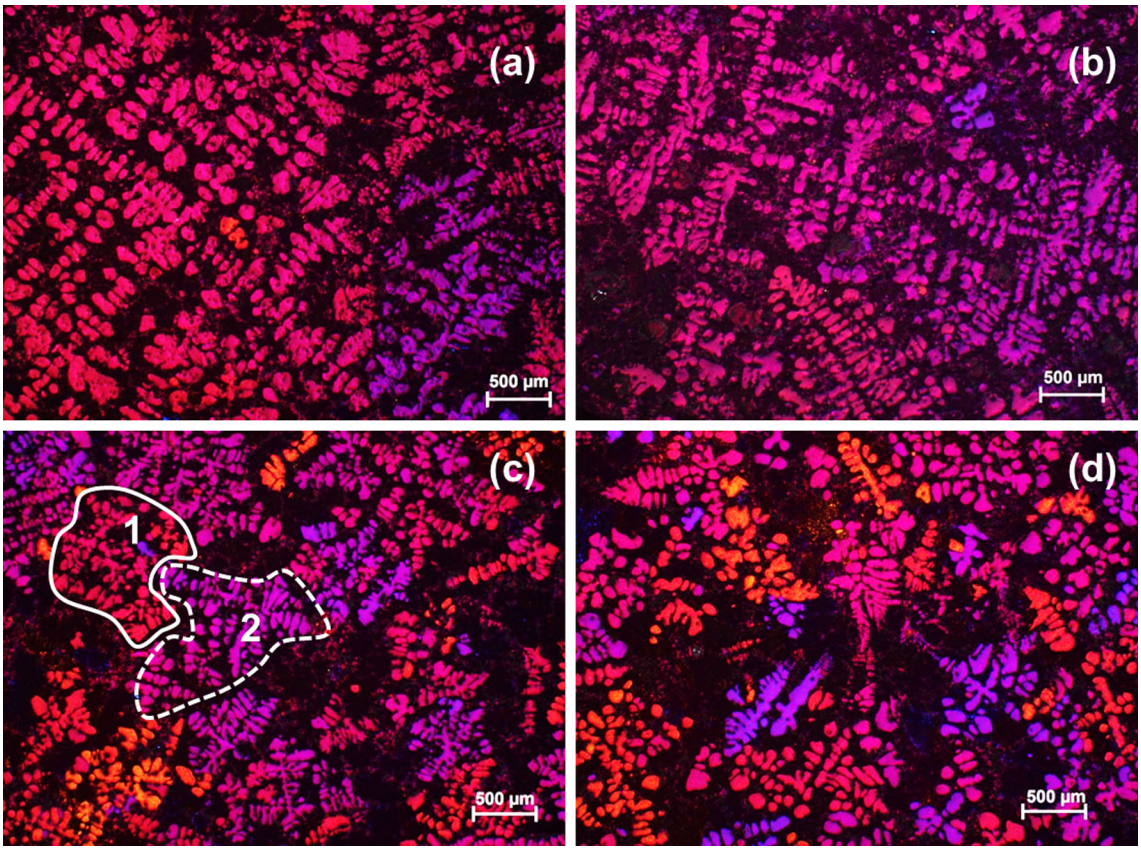

Fig. 4—Grain structures of DC cast billets of A4032 alloy, samples sectioned from the central portion of DC and MC-DC cast billets. (*a*) DC without GR; (*b*) DC with GR; (*c*) MC-DC without GR; and (*d*) MC-DC with GR. As an example, grain 1 and grain 2 are distinguished based on the difference in color (contrast).

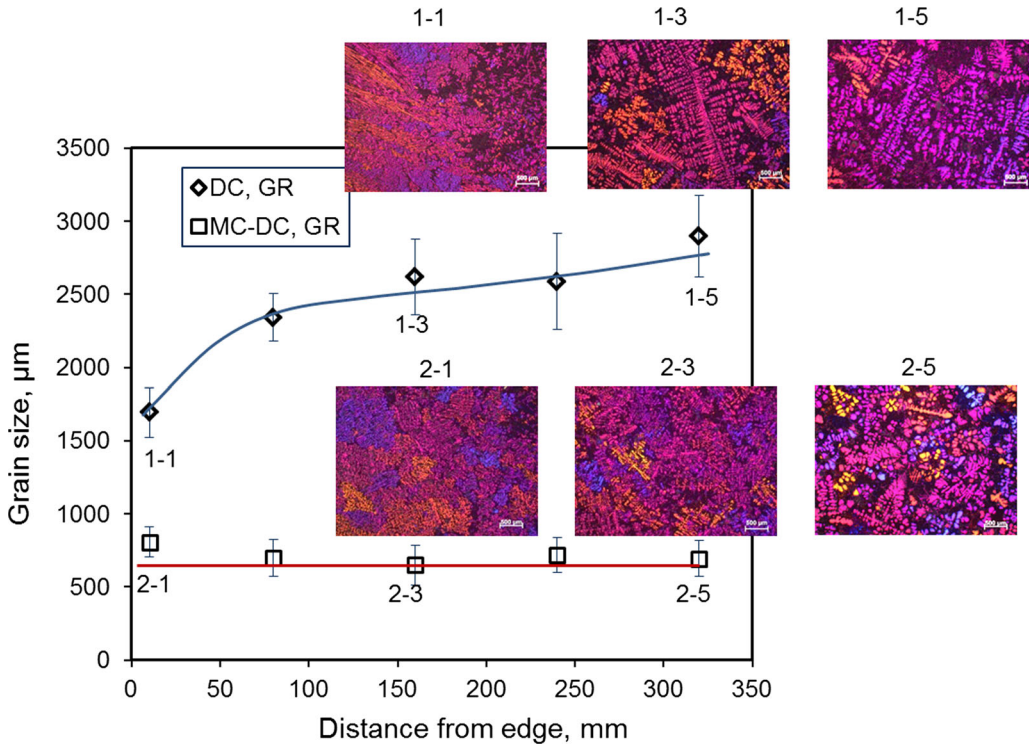

Fig. 5—Quantification of grain size of the α-Al phase in DC and MC-DC cast billets of an A4032 alloy (Note: Grain size refers to the length of dendrite trunks in conventional DC cast billets; for MC-DC cast billets, it is the equivalent size of equiaxed dendritic grains measured by linear intercept technique. The error bar shows the standard deviation. The representative length of scale bar: 500 μm.).

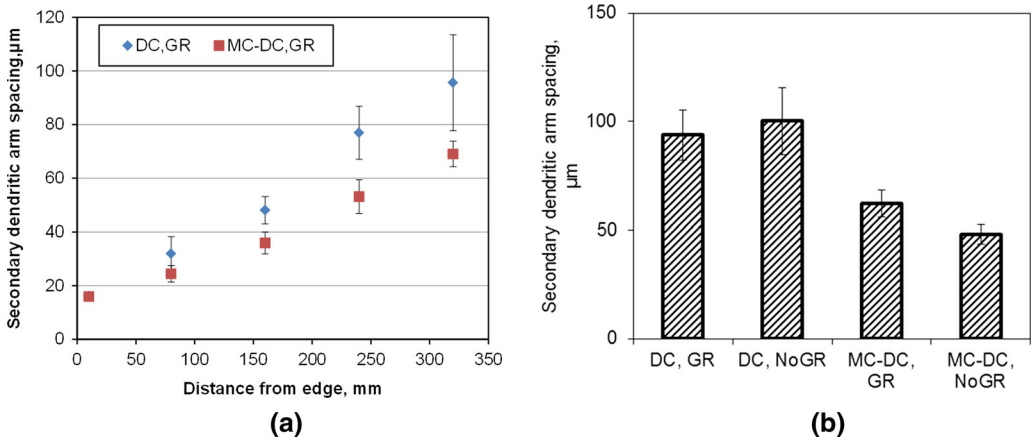

Fig. 6—Refinement of SDAS by MC-DC casting. (*a*) Quantification results of SDAS against distance from the edge of DC and MC-DC cast billets with grain refiner addition (Figs. 3(*b* and *c*)); and (*b*) comparison of SDAS in the central portion of all investigated DC and MC-DC cast billets. The error bar shows the standard deviation.

liquid and solid phases during solidification. The macrosegregation is generally associated with the relative motion of liquid and solid phases in the liquid–solid two-phase zone driven by thermos-solutal convection and solidification shrinkage induced interdendritic flow.[10] The general macrosegregation pattern in a DC cast billet is a negative (solute-depleted) segregation in the center adjoined by positive (solute-rich) segregation approximately at mid-radius with a solute depletion at subsurface followed by strong positive segregation at the surface.[10] In the central portion of a DC cast billet, the shrinkage-driven interdendritic flow dominates the negative segregation, whereas the impact of thermo-solutal convection is reversed and less pronounced.[14] Nevertheless, this effect could be profound when significant penetration of bulk liquid flow enriched in solute into the solid–liquid regions occurs,[37] resulting in channel segregation. In the current study, the occurrence of channel segregation resulted in positive and negative compositional segregation alternately in the central portion of the DC cast billets (Figures 10 and 11). This

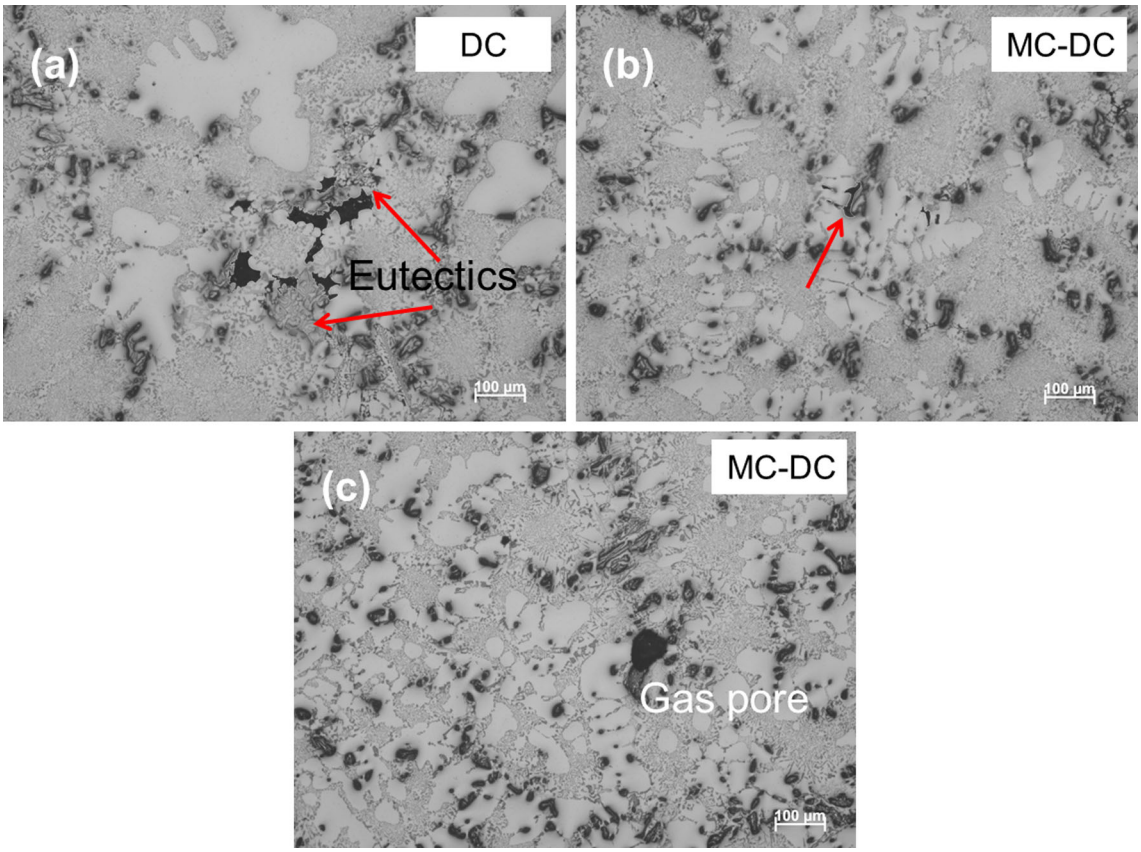

Fig. 7—Characteristics of microporosity observed in (*a*) conventional DC cast billet without grain refiner addition; (*b*) MC-DC cast billet without grain refiner addition; and (*c*) occasionally observed large-sized gas porosity in MC-DC cast billet.

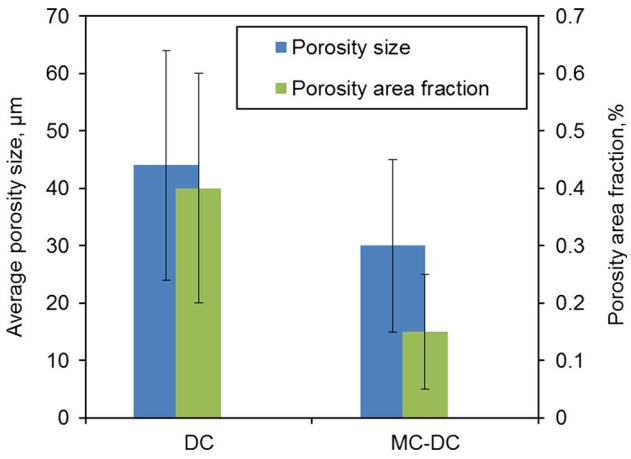

Fig. 8—Comparisons of average size and area fraction of microporosity observed in DC and MC-DC cast billets, performed on images magnified at 100 times the examples shown in Fig. 7. The error bar shows the standard deviation.

is not the case of a typical compositional profile of macrosegregation mentioned earlier.

Channel segregation, also termed "freckles" in directionally solidified superalloys, or "A" or "V" type, segregates in steel castings.[38,39] The name of "freckles" is suggested by the spotted appearance caused by the presence of excess eutectics, second-phase particles, porosity, and small randomly oriented grains. The channel segregation was first proposed to be caused by interdendritic fluid flow resulting from density differences in the liquid by Hunt and co-workers.[40,41] The more open or permeable dendritic mesh requires a smaller buoyancy pressure to allow initiation of channels.[40–44] Flemings and his co-workers developed the concept of flow instability, which occurs at a critical condition of a flow to produce local melting and result in channel segregation.[45,46] Bridge *et al.* and Copley *et al.* investigated the origin of freckles in directionally solidified castings by *in situ* observation providing more direct evidence of the initiation and development of channel segregation.[47,48] A large pocket of liquid is the site where it is most likely for flow instability to occur. It was observed that upward flowing liquid jets cause erosion of the solid–liquid zone and produce dendritic debris. The tendency to freckle is greater in alloys with a large density inversion, high thermal diffusivity, low solute diffusivity, and low viscosity.[48] Mori and Ogi systematically investigated the development of channel segregation using directional solidification of Al-Mg and Al-Mg-Cu alloys.[49] Channel segregation forms when the temperature gradient is below a critical value (Gc). It is concluded that the formation of channel segregation is alloy composition sensitive and thermal condition dependent (in the liquid–solid phase region) during solidification.

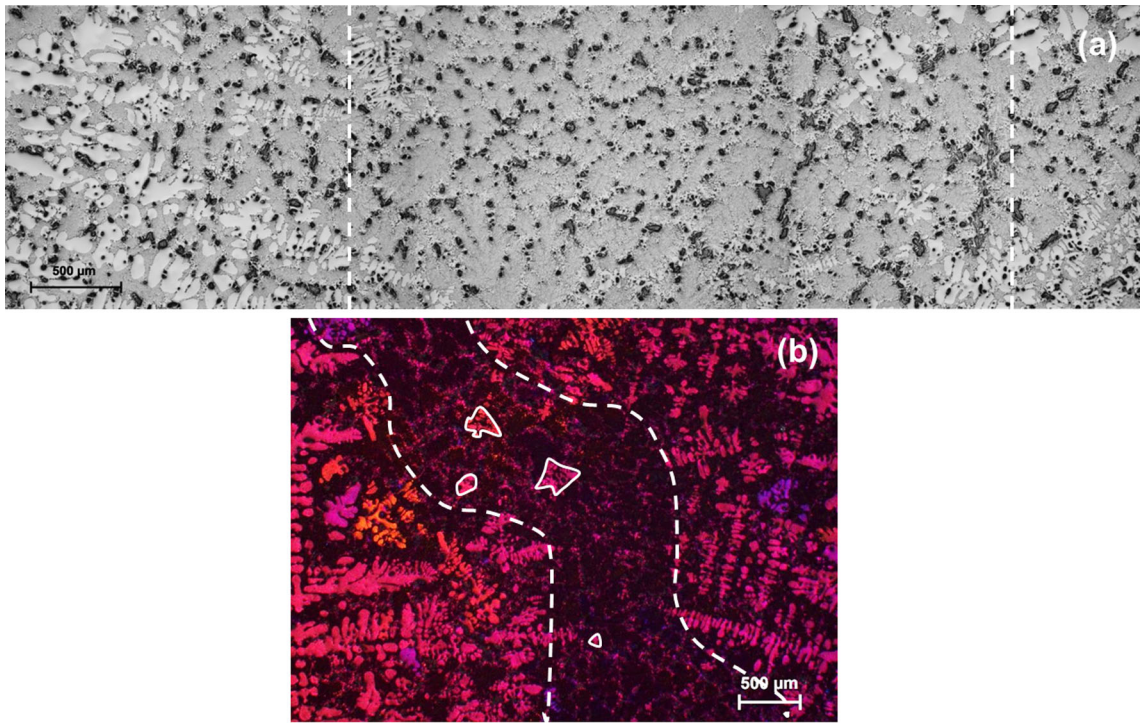

Fig. 9—Channel segregation formed in conventional DC cast billets of an A4032 alloy. (*a*) OM image of the morphology of channel segregation; and (*b*) polarized light image revealing a typical channel segregation zone (within dashed lines), to highlight the feature of a mainly eutectic structure with few dendritic fragments marked with white loops.

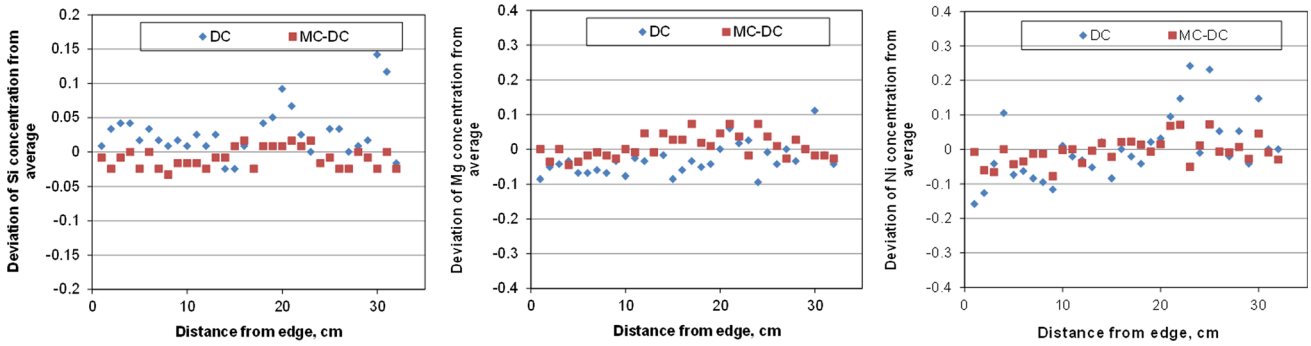

Fig. 10—Compositional profiles of DC and MC-DC castings without grain refiner additions.

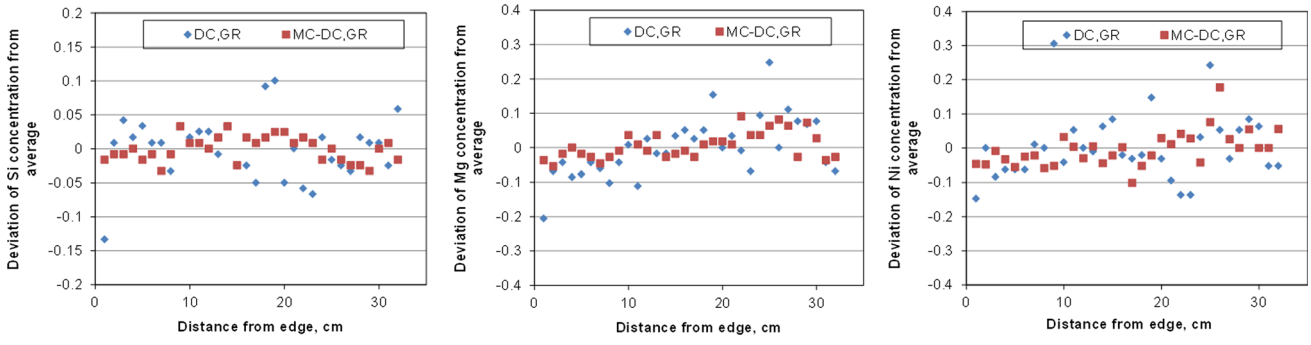

Fig. 11—Compositional profiles of DC and MC-DC castings with grain refiner additions.

Figure 15 shows the concentrations of solute elements in the interdendritic liquid during solidification of an A4032 alloy against the solid fraction calculated by using thermodynamic software based on the Scheil-Gulliver model, in which it is assumed no diffusion in the solid phases, infinitely rapid diffusion in the liquid

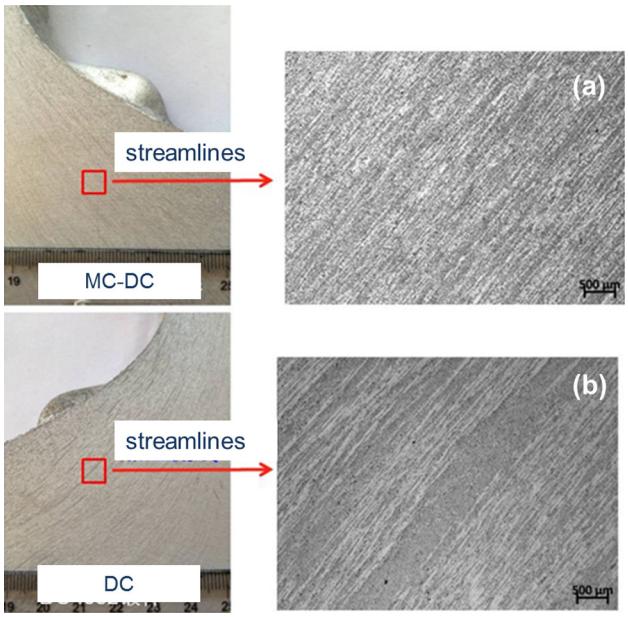

Fig. 12—Fine and uniform structure (forging streamline) of forgings of MC-DC cast billet shown in (*a*), compared with that of conventional DC cast billet with Al-Ti-B-Sr grain refiner addition in (*b*), showing coarse and nonuniform forging streamline.

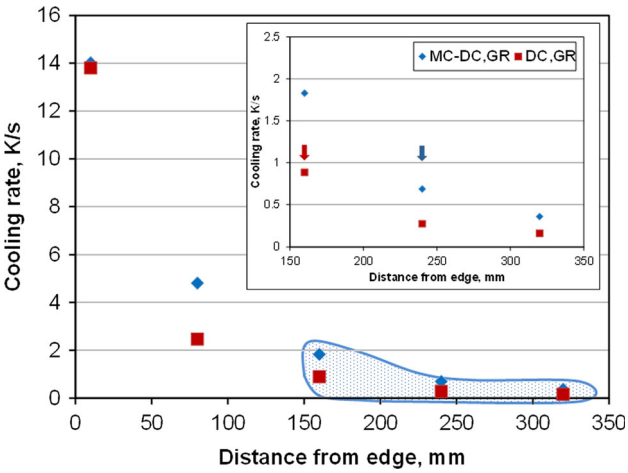

Fig. 13—Estimated cooling rate as a function of the distance from the billets edge based on the measurement results of SDAS shown in Fig. 6(*a*). The shaded area is shown in insert with an enlarged view. Arrows in the insert indicate the position and critical cooling rate where channel segregation was first observed toward the billets center as shown in Fig. 3(*b* and *c*).

phase, and local equilibrium at the solid–liquid interface occur. From Figure 15, one can see severe elemental segregation occurs with the passage of solidification, resulting in enrichment of solute elements in interdendritic liquid. This enrichment of solute elements would result in huge variation of the density of interdendritic liquid. It is therefore critical to control both the liquid pocket size in relation to the initiation and thermal gradient in the sump affecting the development of channel, to prevent the occurrence of channel segregation in DC casting of large-sized billets.

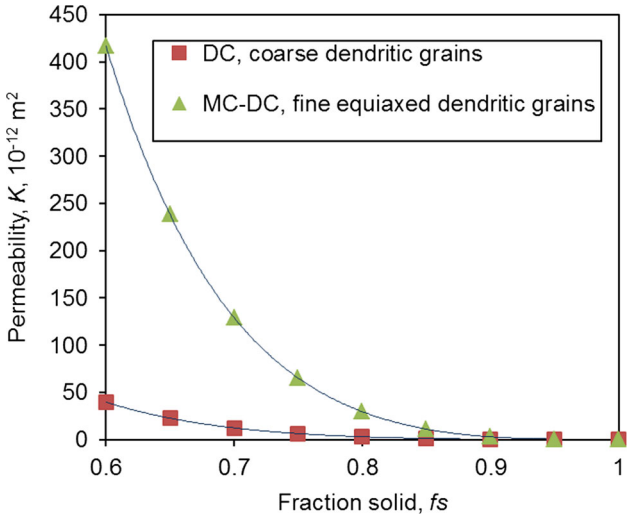

Fig. 14—Estimated value of permeability *K*, of the flow in the mushy zone, based on modified Kozeny–Carman relationship with different grain morphologies.

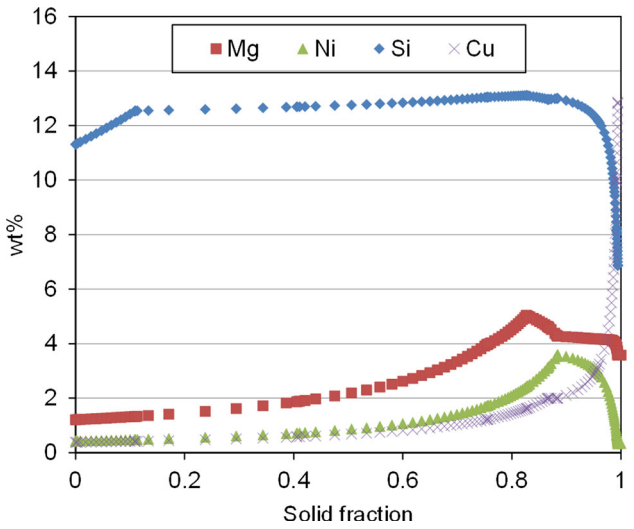

Fig. 15—Solute concentration profile of the interdendritic liquid against solid fraction of A4032 alloy estimated by thermodynamic calculation.

Regarding the prevention of initiation of channel formation, it is desirable to have as small interdendritic liquid pocket as possible to restrain the initiation of channel segregation. In the MC-DC casting, a finer equiaxed dendritic morphology of the primary α-Al phase with finer SDAS (Figure 6) developed. This enables the formation of smaller interdendritic liquid pockets and delays/prevents the initiation of the channel. In the case of conventional DC casting, as a result of the coarse columnar structure, the sizes of interdendritic liquid pockets are much larger than that of MC-DC casting, indicating a more open mesh. This would facilitate the initiation of channel formation.

With intensive melt shearing in the sump, the forced convection in the sump modifies the thermal conditions in the sump. In a previous study on measurement of the

thermal conditions in the sump during MC-DC casting, higher thermal gradient in the liquid–solid region has been determined.[50] In the present study, the calculated results based on SDAS shown in Figure 13 indicate a higher cooling rate in the MC-DC cast billet. Assuming the similar sump profile for both conventional DC and MC-DC casting, the higher cooling rate means a higher thermal gradient. This higher thermal gradient helps prevent the occurrence of channel segregation. The delayed occurrence of channel segregation in the MC-DC cast billet is indicted by a blue arrow in the Figure 13 insert. Under the DC casting conditions in the present study, the critical cooling rate could be around 0.5 to 1 K/s (°C/s) for the channel segregation to happen in the alloy investigated.

In Figure 3, the MC-DC cast billet without grain refiner displays far less channel segregation even when it is compared with the MC-DC cast billet with grain refiner addition. Figure 6(b) shows finer SDAS of the MC-DC cast billet without grain refiner compared with the MC-DC cast billet with grain refiner addition. It suggests the possible role played by the grain structures in the formation of channel segregation and beyond the scope of the present investigation.

V. CONCLUSIONS

MC-DC casting technology has been successfully implemented in the production of industrial-scale DC cast billets to manipulate microstructure and solidification defects by incorporating an intensive melt shearing mechanism in the sump during the DC casting process. Based on detailed investigations on the microstructure and solidification defects in both conventional DC and MC-DC cast billets of an A4032 alloy, the following conclusions can be drawn:

(1) A significant grain refining effect can be achieved by MC-DC casting technology in hard-to-grain-refine Al-Si near eutectic alloy A4032, which is evidenced by coarse columnar dendrites of the α-Al phase in conventional DC cast billets changed to fine equiaxed dendrites in the MC-DC cast billets. The grain refinement is believed to be ascribed to the enhanced heterogeneous nucleation on dispersed oxide particles and fragmentation of dendrites in MC-DC casting, circumventing the poisoning effect on Al-Ti-B grain refiner by the high Si content in the investigated alloy.
(2) A uniform microstructure of the primary α-Al phase with fine secondary dendritic arm spacing can be obtained by MC-DC casting technology. This is understood by the enhanced nucleation and increased cooling rate across the whole cross section resulting from intensive melt shearing in the sump.
(3) An MC-DC cast billet of A4032 alloy shows improvement in macrosegregation. Alleviation/prevention of channel segregation is the dominant mechanism behind the improved macrosegregation. Formation of fine equiaxed dendritic grains and increased local cooling rate by intensive melt shearing in the liquid–solid phase region in the sump suppresses the formation of channel segregation. In the present study, it is concluded that the critical cooling rate could be around 0.5 to 1 K/s (°C/s) for the channel segregation to occur in the investigated alloy.
(4) The reduced porosity area fraction and refined size of microporosity is attributed to the improved permeability and, therefore, to enhanced interdendritic feeding caused by the transition from coarse columnar dendrites in conventional DC cast billets into fine equiaxed dendritic grains in MC-DC cast billets.

ACKNOWLEDGMENTS

The Engineering and Physical Sciences Research Council (EPSRC) of the UK and Chinalco (China) are acknowledged for providing financial support. Dr. F. Gao is gratefully acknowledged for technical assistance with thermodynamic calculations. The valuable and constructive comments and suggestions from reviewers are sincerely appreciated.

OPEN ACCESS

REFERENCES

1. D.G. McCartney: *Int. Mater. Rev.*, 1989, vol. 34, pp. 247–60.
2. A.L. Greer: *Solidification and Casting*, Institute of Physics Publishing, Philadelphia, PA, 2003, p. 214.
3. M.C. Flemings: *Solidification Processing*, McGraw-Hill, New York, 1974.
4. G.K. Sigworth and M.M. Guzowski: *AFS Trans.*, 1985, vol. 93, pp. 907–12.
5. M. Johnsson: *Z. Metallkd*, 1994, vol. 85, pp. 781–85.
6. S.A. Kori, V. Auradi, B.S. Murty, and M. Chakraborty: *Mater. Forum*, 2005, vol. 29, pp. 387–93.
7. Y.C. Lee, A.K. Dahle, D.H. St John, and J.E.C. Hutt: *Mater. Sci. Eng. A*, 1999, vol. 259, pp. 43–52.
8. T.E. Quested: *Mater. Sci. Technol.*, 2004, vol. 20, pp. 1357–69.
9. D. Qiu, J.A. Taylor, M.X. Zhang, and P.M. Kelly: *Acta Mater.*, 2007, vol. 55, pp. 1447–56.
10. R. Nadella, D.G. Eskin, Q. Du, and L. Katgerman: *Prog. Mater. Sci.*, 2008, vol. 53, pp. 421–80.
11. M.C. Flemings: *ISIJ Int.*, 2000, vol. 40, pp. 833–41.
12. C. Beckermann: *Int. Mater. Rev.*, 2002, vol. 47, pp. 243–61.
13. A.V. Reddy and C. Beckermann: *Metall. Mater. Trans. B*, 1997, vol. 28B, pp. 479–89.
14. D.G. Eskin, Q. Du, and L. Katgerman: *Scripta Mater.*, 2006, vol. 55, pp. 715–18.
15. D.G. Eskin and J. Grandfield (Eds.): *Light Metals*. TMS, Warrendale, PA, 2014, pp. 851–60.
16. A. Ludwig, M. Wu, and A. Kharicha: *Metall. Mater. Trans. A*, 2015, vol. 46A, pp. 4854–67.

17. B.J, Zhang, J.Z. Cui, and, G.M. Lu: *Mater. Sci. Eng. A*, 2003, vol. 355, pp. 325–30.
18. D.G. Eskin, A.N. Turchin, and L. Katgerman: *Int. J. Cast Metal Res.*, 2009, vol. 22, pp. 99–102.
19. D.G. Eskin, A. Jafari, and L. Katgerman: *Mater. Sci. Technol.*, 2011, vol. 27, pp. 890–96.
20. Y.B. Zuo, J.Z. Cui, Z.H. Zhao, H.T. Zhang, L. Li, and Q.F. Zhu: *J. Mater. Sci.*, 2012, vol. 47, pp. 5501–08.
21. Z. Fan, B. Jiang, and Y.B. Zuo: PCT/GB2011/051744 UK, 2011.
22. M. Xia, R.A.K. Prasada, and Z. Fan: *Mater. Sci. Forum*, 2013, vol. 765, pp. 291–95.
23. H.T. Li, M. Xia, P. Jarry, G.M. Scamans, and Z. Fan: *J. Cryst. Growth*, 2011, vol. 314, pp. 285–92.
24. Y.B. Zuo, H.T. Li, M.X. Xia, B. Jiang, and Z. Fan: *Scripta Mater.*, 2011, vol. 64, pp. 209–12.
25. H.T. Li, Y. Wang, and Z. Fan: *Acta Mater.*, 2012, vol. 60, pp. 1528–37.
26. Y. Wang, H.T. Li, and Z. Fan: *Trans. Indian Inst. Met.*, 2012, vol. 65, pp. 653–61.
27. J.B. Patel, H.T. Li, M. Xia, S. Jones, S. Kumar, K.A.Q. O'Reilly, and Z. Fan: *Mater. Sci. Forum*, 2014, vol. 794, pp. 149–54.
28. H.T. Li, J.B. Patel, H.R. Kotadia, and Z. Fan: *Mater. Sci. Forum*, 2015, vols. 828–9, pp. 43–47.
29. J. Sengupta, B.G. Thomas, and M.A. Wells: *Metall. Mater. Trans. A*, 2005, vol. 36A, pp. 187–204.
30. R.E. Spear and G.R. Gardner: *Trans. AFS*, 1963, vol. 71, pp. 209–15.
31. D.C. Weckman and P. Niessan: *Metall. Mater. Trans. B*, 1982, vol. 13B, pp. 593–602.
32. W.D. Griffiths and D.G. McCartney: *Mater. Sci. Eng. A*, 1996, vol. 216, pp. 47–60.
33. J. Campbell: *Castings*, 2nd ed., Butterworth-Heinemann, Oxford, 2003, pp. 178–231.
34. P.D. Lee, R.C. Atwood, R.J. Dashwood, and H. Nagaumi: *Mater. Sci. Eng. A*, 2002, vol. 328, pp. 213–22.
35. M. Rappaz, J.M. Drezet, and M. Gremaud: *Metall. Mater. Trans. A*, 1999, vol. 30A, pp. 449–55.
36. D.G. Eskin: *Physical Metallurgy of Direct Chill Casting of Aluminum Alloys*, CRC Press, New York, 2008, p. 134.
37. S.D. Ridder, S. Kou, and R. Mehrabian: *Metall. Trans. B*, 1981, vol. 12B, pp. 435–47.
38. A.F. Giamei and B.H. Kear: *Metall. Trans.*, 1970, vol. 1, pp. 2185–91.
39. G.C. Gould: *Trans. TMS-AIME*, 1965, vol. 233, pp. 1345–51.
40. R.J. McDonald and J.D. Hunt: *Trans TMS-AIME*, 1969, vol. 245, pp. 1993–97.
41. R.J. McDonald and J.D. Hunt: *Metall. Trans.*, 1970, vol. 1, pp. 1787–88.
42. A.K. Sample and A. Hellawell: *Metall. Trans. A*, 1984, vol. 15A, pp. 2163–73.
43. J.R. Sarazin and A. Hellawell: *Metall. Trans. A*, 1988, vol. 19A, pp. 1861–71.
44. A. Hellawell, J.R. Sarazin, and R.S. Steube: *Phil. Trans. R. Soc. Lond. A*, 1993, vol. 345, pp. 507–44.
45. R. Mehrabian, M. Keane, and M.C. Flemings: *Metall. Trans.*, 1970, vol. 1, pp. 1209–20.
46. R. Mehrabian, M. Keane, and M.C. Flemings: *Metall. Trans.*, 1970, vol. 1, pp. 3238–41.
47. M.R. Bridge, M.P. Stephenson, and I. Beech: *Metal. Technol.*, 1982, vol. 9, pp. 429–33.
48. S.M. Copley, A.F. Giamei, S.M. Johnson, and M.F. Hornbecker: *Metall. Trans. B.*, 1970, vol. 1B, pp. 2193–2204.
49. N. Mori and K. Ogi: *Metall. Trans. A*, 1991, vol. 22A, pp. 1663–72.
50. H.-T. Li and Z. Fan: unpublished results, BCAST, Brunel University London, 2017.